Different inhibitory effects by dopaminergic modulation and global suppression of activity

Takuji Hayashi
Department of Applied Physics
Tokyo University of Science

Osamu Araki
Department of Applied Physics
Tokyo University of Science

Tohru Ikeguchi
Department of Information and Mathematical Sciences
Saitama University

***Abstract*— In the dopaminergic network system of prefrontal cortex (PFC)–ventral tegmental area (VTA), physiological experiments have been reported that the D_2 neurons inhibit the spontaneous activity of PFC neurons. However, the functional role of D_2 suppression is not understood well. Is the effect of modulatory D_2 inhibition different from that of GABAergic inhibition? The aim of this research is to reveal the difference between modulatory suppression of D_2 and global inhibition by interneurons. To compare the effects, we construct two alternative models: (1) all GABAergic interneurons of PFC are modulated by a D_2 system, or (2) a global interneuron depolarizes all of PFC pyramidal cells. In computer simulations, we exemplify each of the models using a spiking neural network model with sparse and random synaptic connections. The simulation result shows that model-(1) keeps high correlation between spatial patterns of mean firing rates and the network structure despite the suppression of activity, while model-(2) reduces the correlation. This result suggests that modulatory suppression of D_2 is more than a global suppression and may play a role in memory retrieval function.**

I. Introduction

A lot of experimental data have been shown that ascending projections of midbrain dopamine neurons to prefrontal cortex (PFC) play important roles in working memory and reinforcement learning ([6], [8], [10], for example). These functions are concerned with the dopaminergic mesocortical system, which originates in the ventral tegmental area (VTA) and projects to the neocortex, in particular the prefrontal cortex. It has been shown that electrical and chemical stimulation of the PFC induces burst firing in the VTA dopaminergic neurons [12]. Burst firing of VTA leads to increased DA release at dopaminergic terminals in the forebrain [3].

Generally, DA system is categorized into two groups depending on the receptors: D_1 and D_2 system. The D_1 system in the PFC-VTA networks has been well studied experimentally and from computational models, and it is thought to have intimate relations to the functions such as working memory [4], [5], [6], [8], [10], [11]. On the other hand, the function of D_2 system is not well understood. Electrical stimulation of the VTA leads to a marked inhibition of the spontaneous activity of PFC cells, and this inhibition is mainly due to the activation of the D_2 system rather than to the D_1 [7]. Inhibition of prefrontal cortex might also be due to an indirect action of D_2 on the cortical GABAergic interneurons through increase in release of GABA [9].

As a first step to elucidate the function of D_2 system, we focus on the inhibition of PFC cells through modulatory effects of D_2. Our question is, "Is the effect of modulatory D_2 inhibition different from that of GABAergic inhibition?" The aim of this research is to reveal the difference between modulatory suppression of D_2 and global inhibition by interneurons. To compare the effects, we construct two alternative models: (1) all GABAergic interneurons of PFC are modulated by a D_2 system, we call "PFC-DA model" or (2) a global interneuron depolarizes all of PFC pyramidal cells, we call "PFC-GL model". In the next sections, we explain the details of PFC-DA model and PFC-GL model, respectively. In computer simulations, we exemplify each of the models using a spiking neural network model with sparse and random synaptic connections. The simulation result shows that model-(1) keeps high correlation between spatial patterns of mean firing rates and the network structure despite the suppression of activity, while model-(2) reduces the correlation. The high correlation indicates that internal information stored in the synaptic weights is represented by firing rates. This result suggests that modulatory suppression of D_2 is more than a global suppression and may play a role in memory retrieval function.

II. PFC-DA model

The PFC-DA model consists of PFC neurons and a DA neuron. Fig.1 shows the schematic structure of the PFC-DA model. We constructed PFC network of spiking neural network model with sparse and random synaptic connections [2]. This model is based on the chaotic neural network model, but the output function is the Heaviside function. As such, it is an application and extension of the Nagumo-Sato neuron model. Each neuron receives input spikes from presynaptic neurons and sends spikes to all of its postsynaptic neurons when it fires. After it fires, the neuron becomes more refractory to further firing for a time. Assuming that x_i represents internal activity of each neuron and y_i represents an output value, the dynamics of this model are represented by the following equations:

$$\begin{aligned} x_i(t+1) &= \sum_{j=0}^{N-1}\sum_{r=0}^{t-\Delta_{ij}} \exp\left(-\frac{r}{\tau}\right) s_j w_{ij} y_j(t-r-\Delta_{ij}) \\ &\quad + \sum_{r=0}^{t} \exp\left(-\frac{r}{\tau}\right) A_i(t-r) \\ &\quad - \alpha \sum_{r=0}^{t} \exp\left(-\frac{r}{\tau_{\text{ref}}}\right) y_i(t-r) - \theta \end{aligned} \tag{1}$$

0-7803-7898-9/03/$17.00 ©2003 IEEE

$$y_i(t) = \begin{cases} 1 & \text{if } x_i(t) > 0 \\ 0 & \text{otherwise} \end{cases} \quad (2)$$

where N is the total number of the cells, τ is the decay time constant of the membrane potential, s_j is the discrimination parameter as to whether j cell is excitatory or inhibitory (s_j = 1.0 or -3.0, respectively), w_{ij} is the synaptic weight from j cell to i cell, Δ_{ij} is the delay time of spike transmission from j cell to i cell, $A_i(t)$ is the external input to i cell, α is the scaling parameter of the refractory effect, $\tau_{\rm ref}$ is the decay time constant of the refractory effect, and θ is the resting threshold for firing. For simplicity, time is assume to be discrete. Each cell has an alternative excitatory or inhibitory property, which determines the value of s_j. In the simulations, about 80% of all cells are excitatory, and the rest (20%) are inhibitory. The rate of connections is about 20% in this model, that is, each neuron receives synaptic inputs from about 20% of all neurons except itself(w_{ii} = 0). Transmission delays are randomly selected from limited, discrete values, form 1 to 4 here. The synaptic weights are generally asymmetrical, that is, $w_{ij} \neq w_{ji}$, and of random values in a uniformly distributed range in [0.8,1). We used Poisson process inputs as external inputs. If interspike intervals of the input spikes follow exponential distribution of the probability density in continuous time, such temporal spikes follow the Poisson process. The term Poisson process inputs indicates a temporal series of input signals in which the continuous-time interspike intervals of Poisson process are approximated to the smallest integers not less than the corresponding values. For simplicity, the dopamine neuron in the VTA is assumed to be a simple integrated-and-fire neuron. The dopamine neuron receives spikes from all of PFC pyramidal cells. Thus, the activity of the dopamine neuron reflects populational activity of PFC pyramidal cells. The equation of a DA model is given as follows:

$$x_{\rm DA}(t+1) = \sum_{j_{\rm E}=0}^{N_{\rm E}-1} \sum_{r=0}^{t} \exp(-\frac{r}{\tau_{\rm DA}}) y_{j_{\rm E}}(t-r) \quad (3)$$

where $x_{\rm DA}$ is the internal activity of DA neuron, N_E is the number of the pyramidal neurons in the PFC, and $\tau_{\rm DA}$ is the decay time constant of the membrane potential. For the inhibition of spontaneous activity of PFC cells, GABA interneurons in the PFC enhance the suppressive effect (see Fig.2). Internal activity of DA modulates all of GABAergic inhibition by the following equation:

$$s_j(t+1) = \begin{cases} s_j(t) - \beta x_{\rm DA}(t - \Delta_{\rm DA}) & \text{if } x_{\rm DA}(t) > 0 \\ s_j(t) & \text{otherwise} \end{cases} \quad (4)$$

where β is a scaling parameter whose value is 0.01 in the computer simulations. $\Delta_{\rm DA}$ is the delay time of spike transmission from PFC cell to PFC cell via DA neuron. This s_j rule (Eq.(4)) is applied to every interneuron equally. Fig.2 shows that higher activity of PFC neurons activate the DA neuron and receive suppressive effects within tens of unit time.

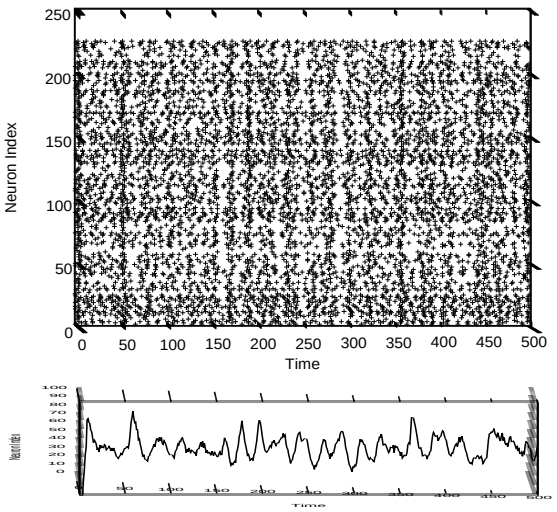

Fig. 2. Raster plots of PFC and internal state of DA model

III. PFC-GL MODEL

The PFC-GL model consists of PFC neurons and a global interneuron (GL) models. PFC model is the same as the PFC network of PFC-DA model. Basically, the behavior of GL model is same as DA model (Eq.(6)).

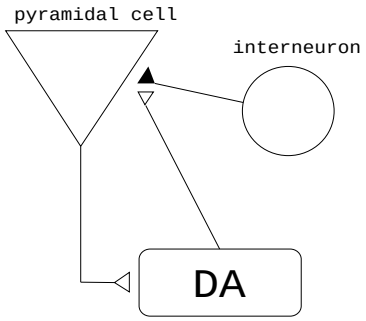

Fig. 1. Schematic structure of PFC-DA model

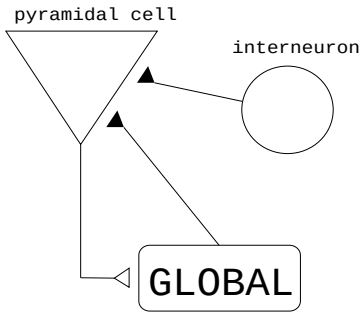

Fig. 3. Schematic structure of PFC-GL model

$$x_i(t+1) = \sum_{j=0}^{N-1}\sum_{r=0}^{t-\Delta_{ij}} \exp(-\frac{r}{\tau})s_j w_{ij} y_j(t-r-\Delta_{ij}) + \sum_{r=0}^{t}\exp(-\frac{r}{\tau})A_i(t-r) - \alpha\sum_{r=0}^{t}\exp(-\frac{r}{\tau_{\text{ref}}})y_i(t-r) - \theta - x_{\text{GL}}(t-\Delta_{\text{DA}}) \quad (5)$$

$$x_{\text{GL}}(t+1) = \sum_{j_{\text{E}}=0}^{N_{\text{E}}-1}\sum_{r=0}^{t}\exp(-\frac{r}{\tau_{\text{GL}}})y_{j_{\text{E}}}(t-r) \quad (6)$$

GL model directly depolarizes all of PFC pyramidal cells. Internal state of PFC pyramidal cells is reduced by internal state of GL model. We observe that GL model changes the internal state similarly as DA model does (see Fig.4 and Fig.2).

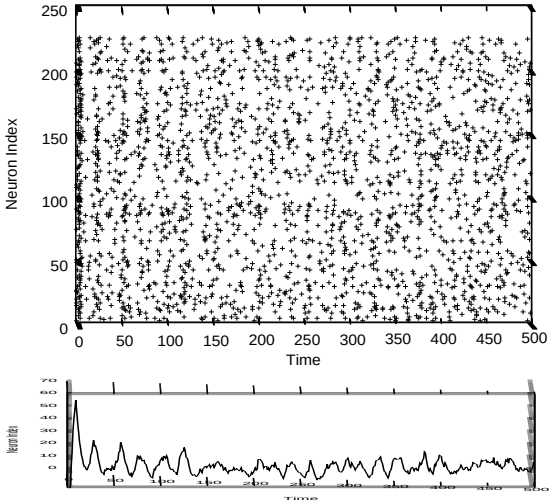

Fig. 4. Raster plots of PFC and internal state of GL model

IV. Computer Simulations

A. Suppressive effect

Fig.5 shows that the suppressive effect by PFC-DA model and PFC-GL model, respectively. In both models, synaptic connection and external input are the same patterns. PFC-DA model and PFC-GL model are more suppressive than PFC model (see Fig.5).

Fig.6 shows spatiotemporal firing patterns and spatial patterns of mean firing rates (SPMFR). Mean firing rate of each neuron in a time window is defined as follows:

$$M_i = \frac{\sum_{t=0}^{T} y_i(t)}{T} \quad (7)$$

SPMFR can be represented using this term M_i as follows:

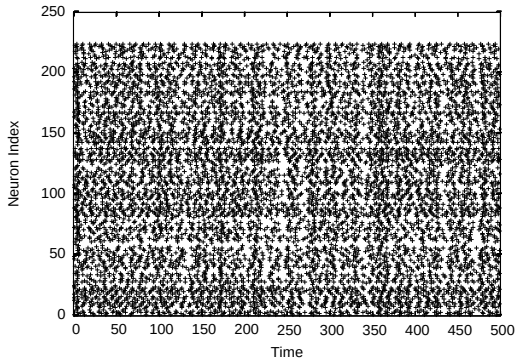

(a) PFC model

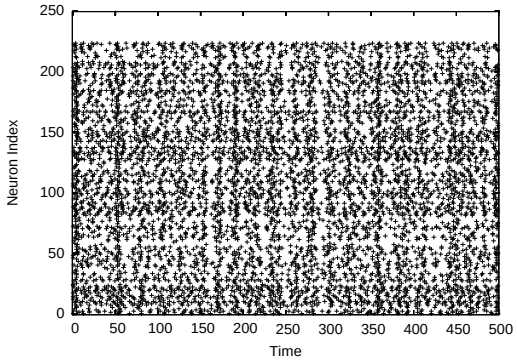

(b) PFC-DA model

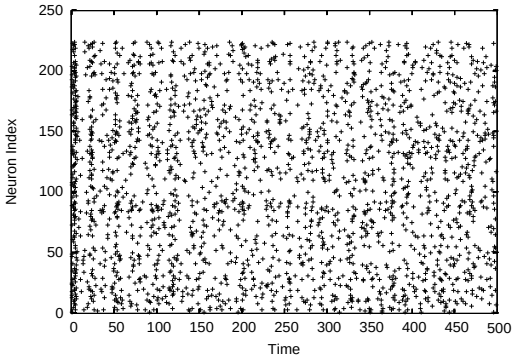

(c) PFC-GL model

Fig. 5. Comparison of suppressive effect

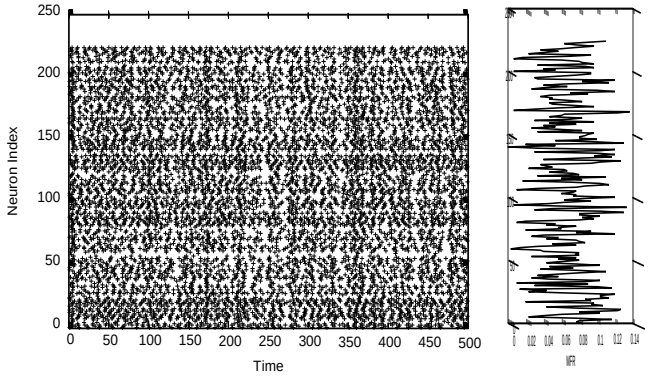

Fig. 6. An example of spatiotemporal firing patterns and spatial patterns of mean firing rates.

$$M = (M_1, M_2, ..., M_N) \tag{8}$$

SPMFR vary with the network and external input pattern. To measure global firing rate over neurons, we defined SPMFR and the average of SPMFR as follows:

$$\text{Ave. of SPMFR} = \frac{\sum_i M_i}{N} \tag{9}$$

Fig.7 shows that average of SPMFR by DA neuron and GL neuron. The error bars indicate standard deviation (SD) (n=100). X-axis indicates average of interspike intervals of the external input. PFC-DA model and PFC-GL model are more suppressive than PFC model (see Fig.5). In addition, the suppressive effect by GL is stronger than that by DA.

B. Correlation coefficient between SPMFR and the W pattern

In the previous study, we showed that the correlation coefficients between SPMFR and the W pattern in this PFC model are close to one in case of relatively higher input frequency. The W pattern is defined as follows:

$$W = (W_1, W_2, ..., W_N) \tag{10}$$

$$W_i = \sum_j s_j w_{ij} \tag{11}$$

W is the spatial patterns of the sum of synaptic weights, in which s_j and w_{ij} are the same variables as in equation (2). The similarity between SPMFR and W means that SPMFR of spikes represent the network structure W. This property of SPMFR reflect can be interpreted as the recall function of internal memory [2].

In order to clarify the difference of suppressive effect, we compared the correlation coefficients between SPMFR and W for PFC-DA and PFC-GL models. Fig.8 shows that correlation coefficient between SPMFR and W of PFC model and PFC-DA model, respectively. Fig.9 shows that correlation coefficient between SPMFR and W of PFC model and PFC-GL model, respectively. The horizontal-axis indicates average

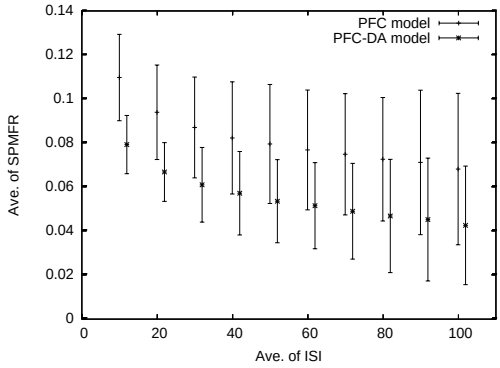

(a) suppression by DA neuron

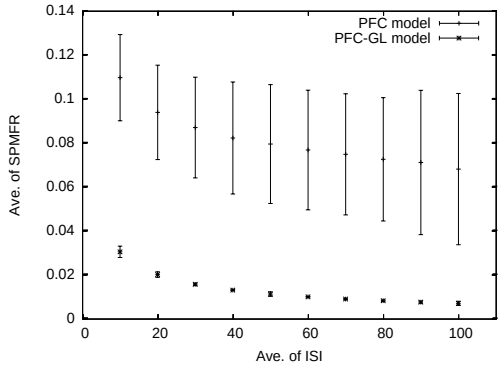

(b) suppression by GL neuron

Fig. 7. Average of SPMFR

of SPMFR, and we calculated correlation coefficients 100 times per one average of ISI. (ave. of ISI = 10,15,20,...,100). The correlation coefficients of PFC-DA and PFC models are almost correspondent (See Fig.8). However, the correlation coefficient of PFC-GL model is lower than PFC model (See Fig.9). This is a remarkable difference between DA and GL inhibitory effects, which we have found. This implies that the DA inhibitory effect suppresses spikes but keeps SPMFR reflecting internal information, while GL inhibition suppresses both of them. Plots of PFC-GL are shifted to the left because of stronger inhibitory effect of GL (See Fig.9).

V. Synaptic weights with attractors

In section IV, we used the synaptic weights of random values in a uniformly distributed range in [0.8). In this section, we examined the difference between DA and GL under the condition that the network dynamics have multiple attractors.

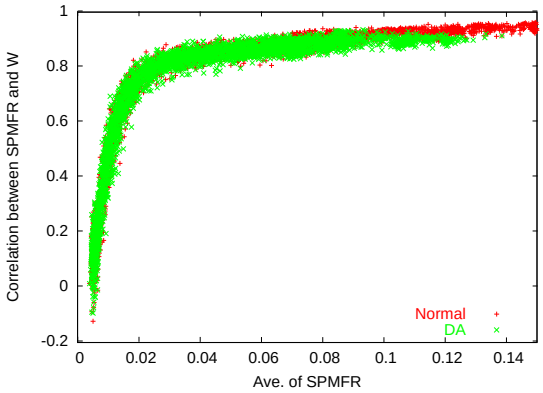

Fig. 8. Correlation between SPMFR and W for PFC and PFC-DA models

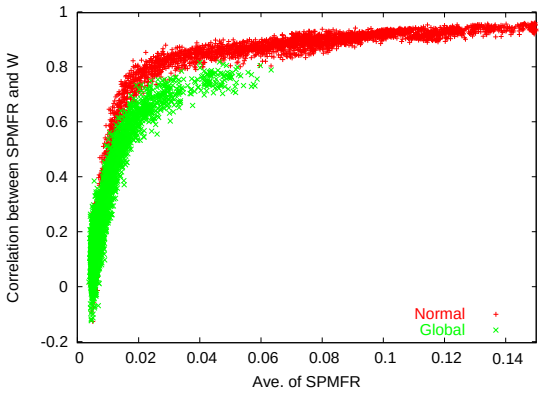

Fig. 9. Correlation between SPMFR and W for PFC and PFC-GL models

We assumed the synaptic weights are given as follows [1]:

$$w_{ij} = \frac{1}{m}\sum_{p=1}^{m}(2x_i^p - 1)(2x_j^p - 1) \qquad (12)$$

where x_i^p is the ith component of the pth stored pattern. And we use four stored patterns ($m = 4$) in this simulation. Fig.10 shows raster plots of PFC-DA model with the synaptic weights defined by Eq.(12), and Fig.11 shows those of PFC-GL model with the same synaptic weights. Since the network dynamics have multiple attractors, SPMFR are itinerant among the stored m patterns in the same way as in the studies so far (for example, [1]). There is a possibility that the itinerancy is chaotic because each neuron model has chaotic properties [2], which we will not examine any more in this study. Since SPMFR are not so stable as those with random synaptic weights, we cannot compare the suppressive effects between PFC-DA and PFC-GL models by calculating correlation coefficients of SPMFR and W as in section IV (Fig.8,9). Thus, we should devise this method for variable SPMFR, or think out another way. This is one of our future works.

VI. Discussion

As average of ISI of external input increases, suppressive effect of both models hardly change, and the average of SPMFR seems to converge. The simulation result shows that PFC-DA model keeps high correlation between spatial patterns of mean firing rates and the network structure despite the suppression of activity, while PFC-GL reduces the correlation. The result suggests that inhibitory effect by dopaminegic modulation may play a role in suppressing noisy signals and memory recall function. In PFC-GL model, the result of correlation coefficient indicates that global suppression may suppress both of recalled memory and other information.

VII. Conclusion

In this research, we constructed two alternative models and revealed the difference between modulatory suppression of D_2 and global inhibition by interneurons. In PFC-DA model, we observe that the activity of PFC pyramidal cells is suppressed and the correlation coefficient between SPMFR and W hardly decreases. The result suggests that dopaminergic modulation may play a role in inhibiting PFC pyramidal cells activity by less spikes for representing internal information.

VIII. Acknowledgment

This research is partially supported by a Grant-in-Aid for Scientific Research on Priority Areas, Advanced Brain Science Project, from Ministry of Education, Culture, Sports, Science and Technology, Japan.

References

[1] M. Adachi and K. Aihara. Associative dynamics in a chaotic neural network. *Neural Networks*, 10(1):83–98, 1997.

[2] O. Araki and K. Aihara. Dual information representation with stable firing rates and chaotic spatiotemporal spike patterns in a neural network model. *Neural Computation*, 13:2799–2822, 2001.

[3] D. B. Carr and Sesack S. R. Projections from the rat prefrontal cortex to the ventral tegmental area: Target specificity in the synaptic associations with mesoaccumbens and mesocortical neurons. *Journal of Neuroscience*, 10:3864–3873, 2000.

[4] D. Durstewitz, M. Kelc, and O. Gunturkun. A neurocomputational theory of the dopaminergic modulation of working memory functions. *Journal of Neuroscience*, 19:2807–2822, 1997.

[5] D. Durstewitz, J. K. Seamans, and T. J. Sejnowski. Neurocomputational models of working memory. *Nat Neurosci*, 3:1184–1191, 2000.

[6] J. R. Hollerman and W. Schultz. Dopamine neurons report an error in the temporal prediction of reward during learning. *Nature Neuroscience*, 1:304–309, 1998.

[7] T. M. Jay, J. Glowinski, and A. M. Thierry. Inhibition of hippocampo-prefrontal cortex excitatory responses by the mesocortical da system. *Neuro Report*, 6:1845–1848, 1995.

[8] P. R. Montague, P. Dayan, and T. J. Sejnowski. A framework for mesencephalic dopamine systems based on predictive Hebbian learning. *Journal of Neuroscience*, 16:1936–1947, 1996.

[9] S. Pirot, R. Godbout, J. Mantz, J. P. Tassin, J. Glowinski, and A. M. Thierry. Inhibitory effects of ventral tegmental area stimulation on the activity of prefrontal cortical neurons: evidence for the involvement of both dopaminergic and gabaergic components. *Neuroscience*, 22:857–865, 1992.

[10] T. Sawaguchi and P. S. Goldman-Rakic. The role of D_1-dopamine receptor in working memory: local injections of dopamine antagonists into the prefrontal cortex of rhesus monkeys performing an oculomotor delayed-response task. *Journal of Neurophysiology*, 71:515–528, 1994.

[11] S. Tanaka. Computational approaches to the architecture and operations of the prefrontal cortical circuit for working memory. *Prog Neuropsychopharmacol Biol Psychiatry*, 25:259–281, 2001.

[12] Z. Y. Tong, P. G. Overton, and D. Clark. Stimulation of the prefrontal cortex in the rat induces patterns of activity in midbrain dopaminergic neurons which resemble natural burst events. *Synapse*, 22:195–208, 1996.

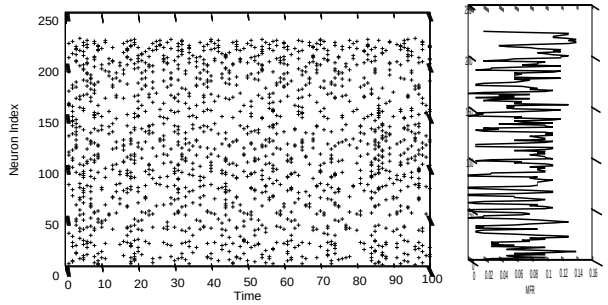

(a) from $t = 0$ to $t = 100$

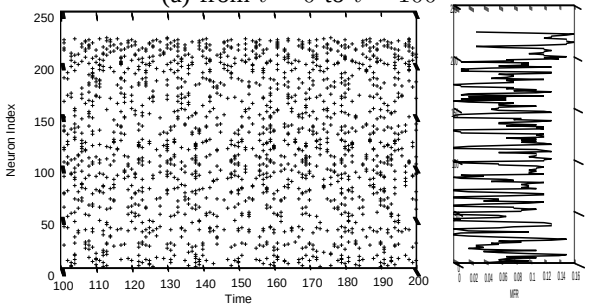

(b) from $t = 100$ to $t = 200$

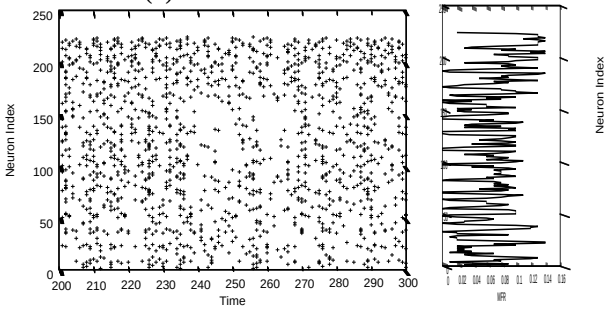

(c) from $t = 200$ to $t = 300$

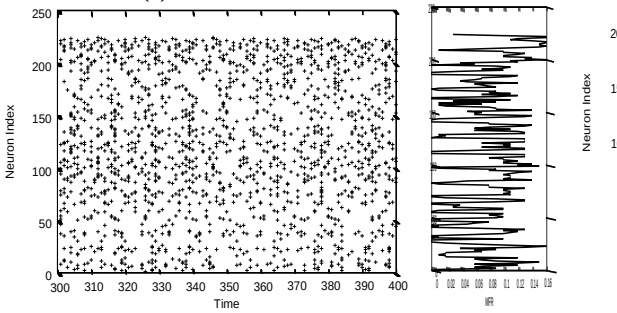

(d) from $t = 300$ to $t = 400$

Fig. 10. Raster plots of PFC-DA model with attractive synaptic weights

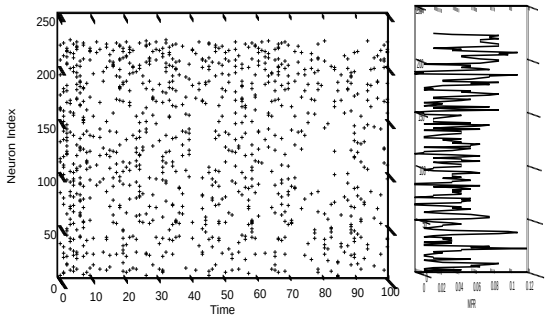

(a) from $t = 0$ to $t = 100$

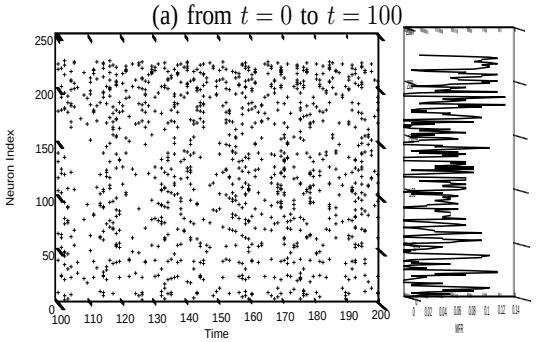

(b) from $t = 100$ to $t = 200$

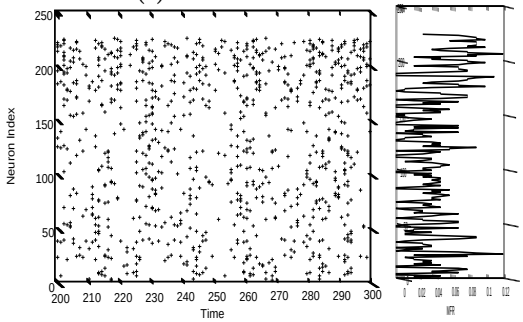

(c) from $t = 200$ to $t = 300$

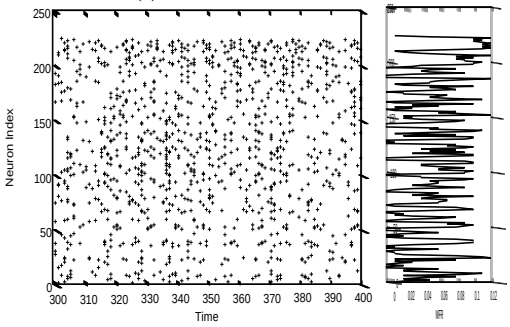

(d) from $t = 300$ to $t = 400$

Fig. 11. Raster plots of PFC-GL model with attractive synaptic weights